ARTICLES

Growth of Prussian Blue Microcubes under a Hydrothermal Condition: Possible Nonclassical Crystallization by a Mesoscale Self-Assembly

Xiao-Jun Zheng, Qin Kuang, Tao Xu, Zhi-Yuan Jiang, Shu-Hong Zhang, Zhao-Xiong Xie,* Rong-Bing Huang, and Lan-Sun Zheng

State Key Laboratory for Physical Chemistry of Solid Surfaces, Department of Chemistry, College of Chemistry and Chemical Engineering, Xiamen University, Xiamen 361005, China

Received: August 6, 2006; In Final Form: January 11, 2007

A classical crystallization process starts from stable nuclei followed by a simple enlargement of the nuclei by unit-cell replication. In recent years, the universality of such classical crystallization has been questioned upon investigations of biomineralization processes, and there are few examples showing that crystal growth may not follow such a classical crystallization process. In this paper, a typical coordination polymer, Prussian blue microcrystals, has been synthesized under hydrothermal conditions. By carefully analyzing the intermediates during the crystal growth process, we found that the growth of Prussian blue under the given growth conditions may follow a nonclassical crystal growth process in which a mesoscale self-assembly of nanocrystallites is included during crystal growth. Such a mesoscale self-assembly process could be a common phenomenon for growth of some crystals with extremely low solubility.

Introduction

Coordination polymers, infinite frameworks consisting of metal ions and bridging ligands, usually have very low solubility in aqueous solution. They have attracted researchers' interests and been thought to be a kind of novel material because of the fascinating properties, rich structures, and potential applications in the fields of catalysis, molecular recognition, sensor, magnetism, photochemistry, etc.[1−4] During the past decade coordination polymers with various structures and properties have been rapidly designed and synthesized. Among the synthesis methods, hydrothermal syntheses become a well-known common method for preparation of coordination polymers. Although the hydrothermal technique is an effective and a powerful method in synthesizing various coordination polymers, the crystal growth process under the hydrothermal condition used to be ignored. Prussian blues (*catena*-[$MFe^{II}[Fe^{III}(CN)_6]\cdot nH_2O$]) (M = cations such as Li^+, Na^+, K^+, etc.) and their analogues, known as molecular magnets, are representative of coordination polymers. The syntheses and magnetic properties of Prussian blues and their analogues have been extensively investigated.[5−7] In this paper, using the growth of Prussian blue (PB) microcrystals under the hydrothermal condition as an example, we show a possible nonclassical crystal growth process for growth of some coordination polymers. A mesoscale self-assembly process has been put forward to account for growth of Prussian blue microcrystals.

A classical crystallization process starts from stable nuclei, followed by a simple enlargement of the nuclei by unit-cell replication through growth of the building blocks such as atoms, ions, molecules, or small clusters on the nuclei surfaces. In recent years, the universality of such classical crystallization has been questioned upon investigations of biomineralization processes.[8] Many biominerals were found to grow through mesoscale self-assembly of defined and monodispersed nanoparticles.[8−11] Furthermore, it has been found that mesoscale self-assemblies are not limited only to biomineralization. Some inorganic and organic nanomaterials were observed to self-assemble into their superstructures.[9,12−14] In addition, some evidence has demonstrated that single crystals may follow a nonclassical growth process involving mesoscale self-assemblies of nanoparticle units. For example,[15] titania nanoparticles can emerge and fuse into highly ordered titania chains and barium sulfate may grow according to a self-assembled aggregation mechanism followed by a fast recrystallization process. These facts suggest that the mesoscale self-assembly process may be another crystallization pathway in formation of some single crystals in normal lab conditions (in contrast to biomineralization). Herein, we show another example for growth of single crystals via a nonclassical growth process. Prussian blue microcrystals were found to grow via a mesoscale self-assembly under the hydrothermal condition. Such a mesoscale self-assembly process could be a common phenomenon for growth of many crystals with extremely low solubility.

Experimental Section

In a typical experiment aqueous $K_3Fe(CN)_6$ solution (0.01 M) and $C_6H_{12}O_6$ solution (0.01 M) were prepared separately. All reagents are analytical grade and used without further purification. Typically, 10 mL of the $K_3Fe(CN)_6$ solution was mixed with 10 mL of the glucose ($C_6H_{12}O_6$) solution, and the mixture was stirred for 10 min. Then, the mixed solution was

* To whom correspondence should be addressed. E-mail: zxxie@xmu.edu.cn.

10.1021/jp065055n CCC: $37.00
Published on Web 03/03/2007

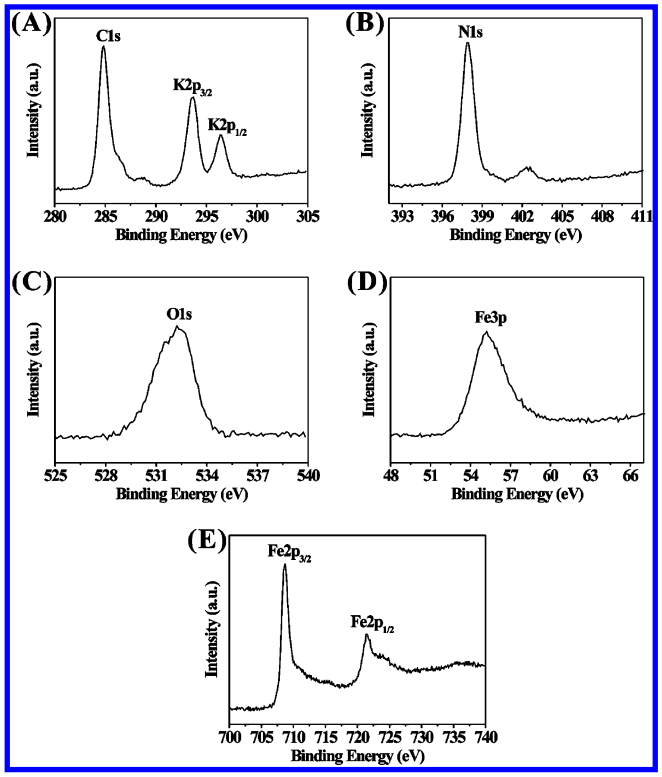

Figure 1. XPS spectra of Prussian blue microcubes obtained at 12 h: (A) C 1s and K 2p; (B) N 1s; (C) O 1s; (D) Fe 3p; (E) Fe 2p. XPS spectra of Prussian blue microcubes proved that the Prussian blue microcubes were composed of elements K, C, N, O, and Fe.

transferred to a Teflon-lined stainless steel autoclave and heated to 120 °C for 12 h. After the reaction, the autoclave was cooled to room temperature naturally, and the product was washed with water and ethanol three times and dried with a vacuum pump at 30 °C for 24 h.

The composition and crystal phase were checked by X-ray photoelectron spectroscopy (XPS, PHI660) and X-ray diffraction (XRD, PANalytical X'pert pro, Cu Kα radiation). Thermogravimetric (TG) analysis was carried out on a NETZSCH STA-449C analyzer. Scanning electron microscopy (SEM) analyses were performed on a LEO1530 microscope with a field-emission electron gun. The high-resolution transmission electron microscopic (HRTEM) observations and selected area electron diffraction were carried out on a FEI TECNAI F30 microscope operated at 300 kV.

Results and Discussion

The chemical compositions of the final products were examined by X-ray photoelectron spectroscopy (XPS), which were composed of elements Fe, K, C, N, and O as shown in Figure 1. The mass loss of lattice water was measured to be 15.0% according to thermogravimetric (TG) analysis. Furthermore, X-ray diffraction (XRD) of the products was measured as shown in the upper part of Figure 2 (line 1). The XRD pattern shows that the products are a pure phase of Prussian blue sharing the same crystal structure of a Prussian blue analogue, $KMnFe(CN)_6 \cdot 2H_2O$ (JCPDS 51-1896). When combining the XPS, TG, and XRD results, a chemical formula of $KFe^{II}Fe^{III}(CN)_6 \cdot 3H_2O$ can be deduced for the as-prepared products. A simulated XRD pattern based on structure information of the Prussian blue analogue was calculated by the Rietveld method using the X'Pert Plus (PANanalytical X'pert) software as shown in the lower part of Figure 2 (line 2), which shows very good agreement between the measured pattern and the simulated one. The refined

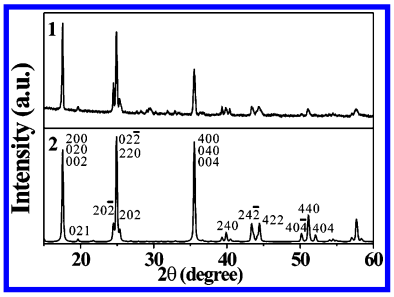

Figure 2. X-ray diffraction pattern of the as-prepared products (line 1) and simulated pattern (line 2) based on the structure information of the isocrystal structure anologue.

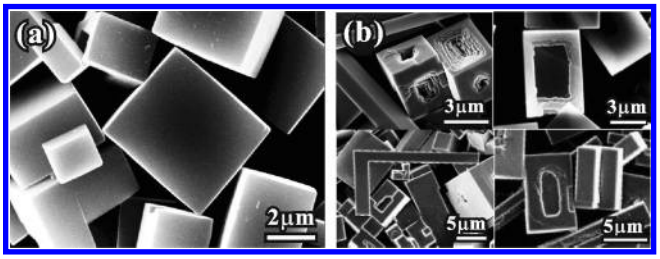

Figure 3. (a) Typical SEM image of Prussian blue microcubes prepared at 120 °C for 12 h. (b) Some particles in the products with irregular shapes such as "L" type, frame, and hollow microcube, in contrast with convex polyhedra, resulted from a classical crystallization.

unit cell of the as-prepared products is monoclinic with cell parameters of $a = 10.085$ Å, $b = 10.125$ Å, $c = 10.111$ Å, and $\beta = 91.97°$. As a result, the Prussian blue $KFe^{II}Fe^{III}(CN)_6 \cdot 3H_2O$ has been successfully prepared by a simple hydrothermal route based on the reaction between $K_3Fe(CN)_6$ and the reductant $C_6H_{12}O_6$. Under hydrothermal conditions, $Fe(CN)_6^{3-}$ could be reduced to $Fe(CN)_6^{4-}$ by $C_6H_{12}O_6$, and at the same time it released the Fe^{3+}, and finally the Prussian blue coordination polymer frameworks were formed successfully.

Figure 3a shows a typical SEM image of the final products for the 12 h heating time. Large amounts of microcubes with a size of several micrometers and very flat surfaces were observed. Such well-faceted morphologies suggest that the cubic particles should be single crystals. The XRD pattern of this product (see Figure 2) shows a very narrow and sharp peak, confirming that the average crystallite size is rather large. As has been well known, naturally grown single crystals via the classical crystal growth route are usually in the shape of convex polyhedra. However, many particles with unusual morphologies such as rectangular frames and microcubes with a rectangular hole were observed in the products as shown in Figure 3b. Such irregular crystallites are difficult to be understood by a classical crystallization process.

To understand the growth mechanism of the Prussian blue crystals, time-dependent experiments were carried out. Figure 4a shows the products after reaction for 40 min. Clearly, the TEM image shows that the products are nanoparticles, most of which are cube shaped and with a size of about 10−20 nm. The high-resolution TEM image (see Supporting Information) shows that the cube-shaped nanoparticles are crystalline, which share the same crystal structure as larger particles grown for a longer reaction time (such as Figure 4d). The nanoparticles are relatively dispersed, although some nanoparticles seem to aggregate and align well with each other. When the reaction time increases to 1.5 h, however, the SEM images of the products do not show well-dispersed enlarged particles as expected. Instead, many particles look like assemblies of nanocubes, where nanocubes are highly oriented with their sides parallel to each other as shown in Figure 4b. From the TEM

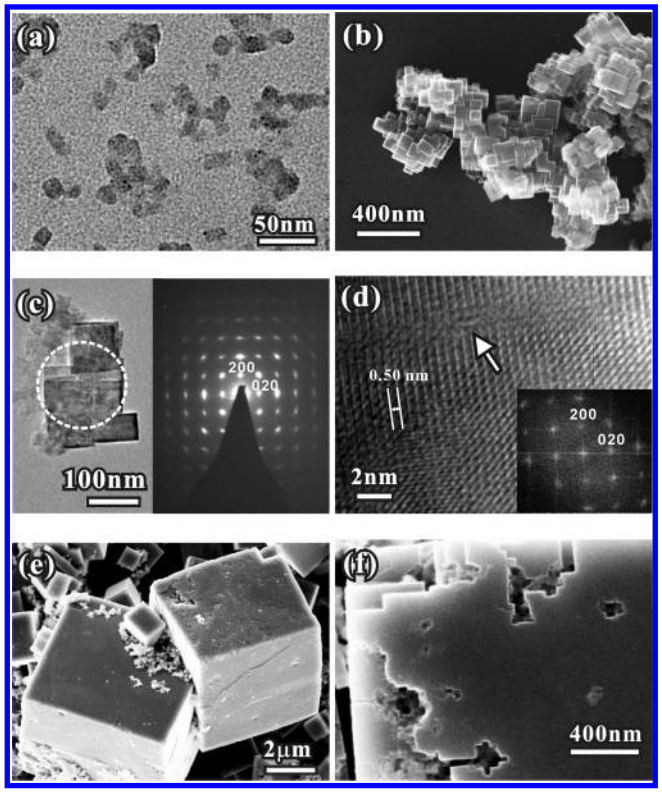

Figure 4. Typical EM images of Prussian blue grown at different growth stages: (a) 40 min (TEM) and (b) 1.5 h (SEM). (c) TEM image of the products of 1.5 h and the corresponding electron diffraction pattern. High-resolution TEM image of the products of (d) 1.5 and (e) 2.5 h (SEM). (f) Enlarged SEM image of the microcube of the products of 2.5 h.

observation of the products, such particles look like mosaic structures as shown in Figure 4c (left). The corresponding SAED pattern is shown in Figure 4c (right), in which all of the diffraction spots can be indexed as diffractions of the [001] zone axis of the Prussian blue phase. The basic two diffraction spots can be indexed as [200] and [020], in agreement with the XRD pattern. However, the diffraction spots are diffusive and elongated to some extent. The result confirms that the nanoparticles are in fact of a mosaic structure in which the mosaic blocks have small orientation deviations. In the high-resolution TEM (HRTEM) image as shown in Figure 4d, the basic lattice spacing measured from the HRTEM image or its Fourier transformation image is about 0.50 nm, corresponding to the spacing of the (200), (020), or (002) lattice planes (as the crystal lattice of the as-prepared Prussian blue is very close to a cube, it is difficult to identify the exact crystal axis from either the high-resolution image or the SAED pattern). Furthermore, the HRTEM also shows some plane defects in the crystal lattice as shown in the upper-left part of Figure 4d and marked by an arrow. When the reaction time increases to 2.5 h, many microcubes with a size of several micrometers can be found. However, the surfaces of the microcubes are quite rough as shown in Figure 4e. Such rough surfaces are very similar to that of many reported mesocrystals.[9] A close look of such rough surfaces (see Figure 4f) shows that many pits and kinks with regular shapes (square or rectangular) appear on the surface. When the reaction time is longer, the surfaces of the grown microcubes are found to become flat (see Figure 3a). By comparing the XRD pattern of the products from a reaction time of 2.5 h and those of 12 h, as shown in Figure 5, it is clearly shown that the diffraction peak becomes narrow with increasing reaction time. In other words, although the particle size of the

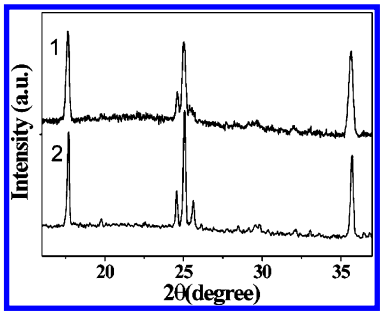

Figure 5. XRD diffraction patterns of Prussian blue grown at different growth stages: (line 1) 2.5 and (line 2) 12 h.

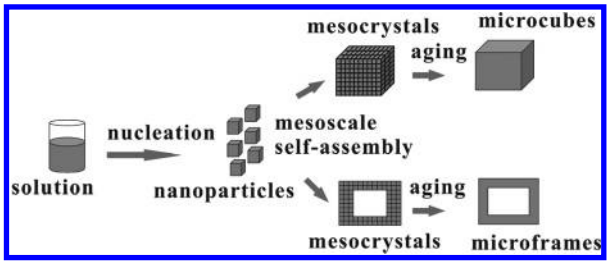

Figure 6. Proposed mechanism for growth of Prussian blue microparticles.

products of 2.5 h is not very different from that of the products of 12 h, the crystallinities between the two products are different. By estimating the crystallite size from the Scherrer formula, it is found that the average crystallite size is about 50 nm for the product of 2.5 h, which is obviously smaller than the apparent particle size observed with SEM. For the case of the product of 12 h, no obviously broaden peak is found.

A crystallization process consists of nucleation and crystal growth. The crystal growth process in the classical mode usually considers a simple enlargement of the nuclei through growth of the building blocks such as the atoms, ions, molecules, or small clusters on the nuclei surfaces. Such a classical crystallization usually results in well-faceted convex polyhedral-shaped particles in all stages of crystallization. Obviously, crystal growth of Prussian blue microcubes does not rigidly follow classical crystallization under our experimental conditions. The SEM and TEM images show that the intermediate particles of the early stage (e.g., 1.5 h of reaction time, Figure 4b−d) during growth of Prussian blue microcrystals are isooriented mosaic structures. The result indicates that the crystal growth process does not follow the simple enlargement of stable nuclei. Very possibly, the intermediate particles with isooriented mosaic structure are via a mesoscale self-assembly process, which aggregation of preformed crystalline building blocks in nanosize is included during crystal growth. Meanwhile, the boundary of the building blocks may fuse together quickly. From the high-resolution image of Figure 4d, we may find a lattice plane defect in the upper-left part. However, this lattice defect does not extend to the right. These facts may indicate that the particle boundaries have fused together during the growth process. Further evidence for the nonclassical crystal growth process comes from the morphologies of intermediates at 2.5 h, where the rough surfaces in fact consist of a large amount of regular polyhedral kinks or pits. Such high-density temporary defects are difficult to appear if the classical crystal growth process is adopted. However, by a mesoscale assembly process, it becomes possible.

On the basis of the above experimental evidence, a growth mechanism via mesoscale self-assembly is proposed as illustrated in Figure 6. At the beginning, the Prussian blue nuclei generate and grow into nanocrystallite intermediates. In this

process the extremely low solubility of the Prussian blue allows formation of large quantities of nanocrystallites because it is very easy for the system to reach the highly supersaturated condition and it nucleates into nanocrystallites. Furthermore, the low solubility of the product may prevent the occurrence of the Ostward ripening process usually taking place in classical crystal growth (in present case, the reductant glucose may also play the role of nanocrystallite stabilizer), by which some nuclei dissolve during growth of the other stable nuclei. Instead, the primary nanocrystallites aggregate to form well-oriented or even isooriented mosaic intermediates. On the other hand, on the crystallite surfaces of Prussian blue, CN groups very possibly exist. During the growth and aging process (keeping a high temperature under the hydrothermal process for more than 10 h), the boundaries of the adjacent nanocrystallites fuse together by reacting with Fe^{3+} ions released from the reactant $Fe(CN)_6^{3-}$. As a result, the average crystallite size becomes larger during the aging process, as proved by the XRD pattern of Figure 5. Similar aging processes also take place during the biomineralization process; as an example, one may find transformation of surface hydroxy (−OH) to oxo (−O−) bridges between two neighbor oxide particles by releasing H_2O during the biomineralization process.[8,11]

Being different from the classical crystallization process, the mesoscale self-assembly results from the assemblies of defined and monodispersed nanoparticles.[9−11] Such mesoscale self-assembly is a key process in biomineralization.[16,17] H. Cölfen and M. Antonietti predicted that mesocrystal formation processes may even be a common crystallization pathway in formation of single crystals in concluding remarks of their recent review about mesocrystals.[9] Growth of Prussian blue microcubes in our case should be a typical example of nonclassical growth of single crystals, especially for those having extremely low solubility.

In conclusion, through analyzing the products of the different stages during the crystal growth process of Prussian blue microcubes under the hydrothermal condition, a mesoscale self-assembly followed by fusing the adjacent crystallites has been put forward to account for the growth mechanism of the Prussian blue microcrystals. Such a modified mesoscale self-assembly process could be a common phenomenon for the growth of some crystals with extremely low solubility.

Acknowledgment. This work was supported by the National Natural Science Foundation of China (grant nos. 20673085, 20473069, and 20671078), the Key Scientific Project of Fujian Province of China (grant no. 2005HZ01-3), NCET from the Ministry of Education of China, and the Fok Ying-Tung Educational Foundation.

Supporting Information Available: High-resolution TEM image of the nanocube product grown with a reaction time of 40 min. This material is available free of charge via the Internet at http://pubs.acs.org.

References and Notes

(1) Hagrman, P. J.; Hagrman, D.; Zubieta, J. *Angew. Chem., Int. Ed.* **1999**, *38*, 2638.
(2) Moulton, B.; Zaworotko, M. J. *Chem. Rev.* **2001**, *101*, 1629.
(3) Yaghi, O. M.; O'Keeffe, M.; Ockwig, N. W.; Chae, H. K.; Eddaoudi, M.; Kim, J. *Nature* **2003**, *423*, 705.
(4) Zaworotko, M. J. *Chem. Commun.* **2001**, 1.
(5) Verdaguer, M.; Bleuzen, A.; Marvaud, V.; Vaissermann, J.; Seuleiman, M.; Desplanches, C.; Scuiller, A.; Trian, C.; Garde, R.; Gelly, G.; Lomenech, C.; Rosenman, I.; Veillet, P.; Cartier, C.; Villain, F. *Coord. Chem. Rev.* **1999**, *190−192*, 1023.
(6) (a) Vaucher, S.; Li, M.; Mann, S. *Angew. Chem., Int. Ed.* **2000**, *39*, 1793. (b) Yang, J.; Wang, H.; Lu, L.; Shi, W.; Zhang, H. *Cryst. Growth Des.* **2006**, *6*, 2438.
(7) (a) Zhou, P. H.; Xue, D. S.; Luo, H. Q.; Chen, X. G. *Nano Lett.* **2002**, *2*, 845. (b) Johansson, A.; Widenkvist, E.; Lu, J.; Boman, M.; Jansson, U. *Nano Lett.* **2005**, *5*, 1603. (c) Vaucher, S.; Fielden, J.; Li, M.; Dujardin, E.; Mann, S. *Nano Lett.* **2002**, *2*, 225. (d) Uemura, T.; Kitagawa, S. *J. Am. Chem. Soc.* **2003**, *125*, 7814. (e) Sun, H. L.; Shi, H. T.; Zhao, F.; Qi, L. M.; Gao, S. *Chem. Commun.* **2005**, 4339.
(8) Banfield, J. F.; Welch, S. A.; Zhang, H.; Ebert, T. T.; Penn, R. L. *Science* **2000**, *289*, 751.
(9) Cölfen, H.; Antonietti, M. *Angew. Chem., Int. Ed.* **2005**, *44*, 5576.
(10) Bowden, N.; Terfort, A.; Carbeck, J.; Whitesides, G. M. *Science* **1997**, *276*, 233.
(11) Cölfen, H.; Mann, S. *Angew. Chem., Int. Ed.* **2003**, *42*, 2350.
(12) Clark, T. D.; Tien, J.; Duffy, D. C.; Paul, K. E.; Whitesides, G. M. *J. Am. Chem. Soc.* **2001**, *123*, 7677.
(13) Li, M.; Lebeau, B.; Mann, S. *Adv. Mater.* **2003**, *15*, 2032.
(14) Kulkarni, G. U.; Thomas, R. J.; Rao, C. N. R. *Pure Appl. Chem.* **2002**, *74*, 1581.
(15) (a) Penn, R. L.; Banfield, J. F. *Geochim. Cosmochim. Acta* **1999**, 63, 1549. (b) Alivisatos, A. P. *Science* **2000**, *289*, 736. (c) Judat, B.; Kind, M. *J. Colloid Interface Sci.* **2004**, *269*, 341.
(16) Kniep, R.; Busch, S. *Angew. Chem., Int. Ed.* **1996**, *35*, 2624.
(17) (a) Mann, S. *Chem. Commun.* **2004**, 1. (b) Taden, A.; Landfester, K.; Antonietti, M. *Langmuir* **2004**, *20*, 957. (c) Simon, P.; Schwarz, U.; Kniep, R. *J. Mater. Chem.* **2005**, *15*, 4992. (d) Weiner, S.; Addadi, L. *J. Mater. Chem.* **1997**, *7*, 689.